

A NEW METHOD FOR THE PREDICTION OF GIBBS FREE ENERGIES OF FORMATION OF PHYLLOSILICATES (10 Å AND 14 Å) BASED ON THE ELECTRONEGATIVITY SCALE

PHILIPPE VIEILLARD

UMR-CNRS 6532 Hydr'ASA*, 40 ave du Recteur Pineau, 86022 Poitiers Cedex, France

Abstract—The method for prediction of Gibbs free energies of formation, based on the parameter $\Delta_G O^{\ominus} M^{z+}(\text{clay})$ characterizing the oxygen affinity of the cation M^{z+} , on the smectites, considered as hydrated clay minerals, has been used for micas and brittle micas, and yielded underestimated values. This method of prediction can be improved by a new set of parameters $\Delta_G O^{\ominus} M^{z+}(\text{clay})$, characterizing the electronegativity of a cation in a specific site (interlayer, octahedral, tetrahedral in the 10 Å minerals), determined by minimizing the difference between experimental Gibbs free energies and calculated Gibbs free energies of formation from constituent oxides. By considering the crystal structure of 10 Å and 14 Å minerals, and assuming the same electronegativity of cations, $\Delta_G O^{\ominus} M^{z+}(\text{o})$, in the octahedral sheets, an attempt is made to determine the electronegativity of cations in the brucitic sheet, $\Delta_G O^{\ominus} M^{z+}(\text{b})$. The results indicate that this prediction method compared to other determinations, gives values within 0.25% of the experimentally-estimated values. The relationships between $\Delta_G O^{\ominus} M^{z+}(\text{clay})$ corresponding to the electronegativity of a cation in the interlayer, octahedral, tetrahedral or brucitic sites and known $\Delta_G O^{\ominus} M^{z+}(\text{aq})$ were thus determined, allowing the determination of the electronegativity of transition metal ions and trivalent ions in each of the four sites and consequently contribute to the prediction of Gibbs free energies of formation of different micas and chlorites. Examples are given for low-Fe clinocllore whose solubility is measured experimentally and the results appear excellent when compared with experimental values.

Key Words—Amesite, Bityite, Chamosite, Chlorites, Clinocllore, Clintonite, Cookeite, Cronstedtite, Dombassite, Gibbs Free Energies of Formation, Hendricksite, Kinoshitalite, Lepidolite, Micas, Polyolithionite, Preiswerkite, Ripidolite, Sudoite, Taeniolite, Zinnwaldite

INTRODUCTION

Phyllosilicate minerals are classified in three different groups: micas (pyrophyllite, muscovite and brittle micas); chlorites (clinocllore, chamosite, sudoite, cookeite); and 7 Å minerals (kaolinite, lizardite, nepouite) are considered to be well crystallized compounds and are not hydrated. Smectites are 2:1 type layer silicates with an expandable structure carrying a certain amount of water and excess negative charge.

Recently a new method of prediction of Gibbs free energies of formation was devised for hydrated clay minerals (Vieillard, 2000) and gave excellent agreements with calculated Gibbs free energies from solubility measurements. The principle is based on several concepts. The poorly crystallized clay minerals are assumed to be fully hydrated and are all of the same particle size (not the same volume because of variable amounts of water in the interlayer spaces of swelling clays). The Gibbs free energy of formation from constituent oxides is the sum of the products of the molar fraction of an O atom bound to any two cations multiplied by the electronegativity difference defined by the $\Delta_G O^{\ominus} M^{z+}(\text{clay})$ between any two consecutive

cations. The $\Delta_G O^{\ominus} M^{z+}(\text{clay})$ value, using a weighting scheme involving the electronegativity of a cation in a specific site (interlayer, octahedral and tetrahedral) is assumed to be constant and can be calculated by minimizing the difference between experimental Gibbs free energies (determined from solubility measurements) and calculated Gibbs free energies of formation from constituent oxides.

Micas and brittle micas have variable compositions. Interlayer cations may be occupied by alkaline cations (Na^+ , K^+ , Rb^+ and Cs^+) and alkaline earth cations (Ca^{2+} , Sr^{2+} and Ba^{2+}). Cations such as Li^+ , Mg^{2+} , Al^{3+} , transition metal ions such as Fe^{2+} , Fe^{3+} , V^{3+} , Mn^{2+} , Mn^{3+} , Zn^{2+} , Cr^{3+} or Ti^{4+} may fill the octahedral sites. Cations such as Fe^{3+} and Be^{2+} can be located in tetrahedral sites, usually occupied by Al^{3+} and Si^{4+} .

Chermak and Rimstidt (1989) proposed a method of prediction of Gibbs free energies of formation for some classical micas but gave very high errors of prediction for celadonite and brittle micas (difference of 50 kJ mol⁻¹ between experimental and predicted Gibbs free energies of formation).

The prediction of Gibbs free energies of micas using the method developed by Vieillard (2000) led systematically to underestimated values for all micas (the difference between predicted and experimental Gibbs free energies of formation ranges from 14 kJ mol⁻¹ in

* E-mail address of corresponding author: philippe.vieillard@hyd.rasa.univ-poitiers.fr

paragonite to 36 kJ mol^{-1} in phlogopite) and brittle micas (ranges from 6 kJ mol^{-1} in siderophyllite to 30 kJ mol^{-1} in eastonite). This means that the values of the parameter $\Delta_G O^=M^{z+}(\text{clay})$ in interlayer, octahedral and tetrahedral sites, initially assumed to be hydrated clay minerals, are not suited for well-crystallized, large grain-size micas. The first part of this paper aims to redetermine the electronegativity scale for interlayer and octahedral sites in micas, necessary to predict Gibbs free energies of formation of some micas like biotite, kinoshitalite, hendricksite, bityite, anandite, zinnwaldite, chernykhite and preiswerkite.

At present there is no accurate method for the prediction of Gibbs free energies of formation for chlorite minerals. Those of Chermak and Rimstidt (1989) and Nriagu (1975) produce very large errors. Several activity-composition models have been proposed to model compositional variation in the chlorite group of minerals (Stoessell, 1984; Walshe, 1986; Aagaard & Jahren, 1992; Holland *et al.*, 1998). All these authors proposed a model based on six end-member minerals considered as ideal phases, for which experimental data were lacking.

From the new relationship between $\Delta_G O^=M^{z+}(\text{clay})$ corresponding to the electronegativity of a cation in octahedral sites and known $\Delta_G O^=M^{z+}(\text{aq})$ in micas, obtained in this work, the second part of this paper will relate to the determination of a new set of values of $\Delta_G O^=M^{z+}(\text{clay})$ in brucitic sheets, by minimizing the difference between calculated and theoretical Gibbs free energy of formation from oxides of chlorites. So, prediction of Gibbs free energies of formation of chlorites with various cations located both in octahedral and brucitic sites will be possible, when we know the electronegativity of the cation in octahedral and brucitic sites.

METHODOLOGY

The method of prediction of Gibbs free energy of formation of clays minerals is based on the parameter $\Delta_G O^=M_i^{z_i+}(\text{aq})$ as defined initially by Tardy and Garrels (1976, 1977), Tardy and Gartner (1977) and Tardy and Vieillard (1977). An historical development of the parameter $\Delta_G O^=M_i^{z_i+}$ was presented by Vieillard (2000).

Gibbs free energies of formation from constituent oxides, $\Delta G_{\text{ox}}^{\circ}$

Consider a layer silicate containing continuous two-dimensional tetrahedral sheets of composition T_2O_5 (T = tetrahedral cation, normally Si, Al or Fe^{3+}). Two kinds of chemical formula are considered here depending on the layer type and type of interlayer. (a) 2:1 layer type, $(M_{1_i})(M_{o_j})(\text{Si}_{(4-t)}\text{Al}_t)\text{O}_{10}(\text{OH})_2$ (with l_i the number of interlayer atom which varies from 0 (pyrophyllite, talc) to 1 (micas, if $M = \text{K}^+$ or Na^+ , brittle micas, if $M = \text{Ca}^{2+}$, or Ba^{2+}). (b) 2:1:1 layer type, $(M_{o_j})(\text{Si}_{(4-t)}\text{Al}_t)\text{O}_{10}(\text{OH})_2 \cdot (M_{b_k})(\text{OH})_6$ where b_k is the number of brucitic cations.

Interlayer sites may be occupied by cations such as Li^+ , Na^+ , K^+ , Ca^{2+} and Ba^{2+} . Octahedral sites and brucitic sites are, to a limited extent, occupied by cations such as Li^+ , Mg^{2+} , Al^{3+} , Fe^{3+} and several cations belonging to the transition series. The Gibbs free energy of formation of a phyllosilicate, ΔG_f° (phyllosilicate), is a stoichiometric summation of Gibbs free energies of formation of the different constituent oxides and a second term, $\Delta G_{\text{ox}}^{\circ}$, designating Gibbs free energies of formation from constituent oxides:

$$\Delta G_f^{\circ}(\text{phyllosilicates}) = \sum_{i=1}^{i=n_s} (n_i) \Delta G_f^{\circ}(M_i O_x) + \Delta G_{\text{ox}}^{\circ} \quad (1)$$

where the Gibbs free energies of formation of the oxides are given in Table 1.

The Gibbs free energy of formation from the oxides, $\Delta G_{\text{ox}}^{\circ}$ is calculated by the following equation, which is analogous to those of the enthalpy of formation given by Vieillard (1994a):

$$\Delta G_{\text{ox}}^{\circ} = -N \left[\sum_{i=1}^{i=n_s-1} \sum_{j=i+1}^{j=n_s} X_i X_j \left(\Delta_G O^=M_i^{z_i+}(\text{clay}) - \Delta_G O^=M_j^{z_j+}(\text{clay}) \right) \right] \quad (2)$$

where X_i and X_j are the molar fractions of oxygen related to the cations $M_i^{z_i+}$ and $M_j^{z_j+}$, respectively, in the individual oxides $M_i O_{x_i}$ and $M_j O_{x_j}$, relative to the bulk number of oxygen of the mineral, N :

$$X_i = (1/N)(n_i x_i) \quad (3)$$

$$X_j = (1/N)(n_j x_j) \quad (4)$$

where N is the total number of O atoms of all oxides, *i.e.* the bulk number of oxygen or the compound:

$$\sum_{i=1}^{i=n_s} = N \quad (5)$$

The parameters $\Delta_G O^=M_i^{z_i+}(\text{clay})$ and $\Delta_G O^=M_j^{z_j+}(\text{clay})$ characterize the electronegativity of cations $M_i^{z_i+}$ and $M_j^{z_j+}$ respectively, in a specific site. These terms are initially dependent on structural parameters such as bond length, average bond length, and polarizability (Vieillard, 1982, 1994a,b; Vieillard and Tardy, 1988a) and they are assumed to be constant here.

In micas, *e.g.* muscovite, the Al^{3+} ion, located in two sites, octahedral or hydrated sites (index o) and tetrahedral sites (index t), have different structural surroundings. This implies that terms such as $\Delta_G O^=\text{Al}^{3+}(\text{o})$ and $\Delta_G O^=\text{Al}^{3+}(\text{t})$, are characteristic of the electronegativity of the ion Al^{3+} in two different sites and are not equal. Similarly, octahedral aluminum $\Delta_G O^=\text{Al}^{3+}(\text{o})$, tetrahedral aluminum $\Delta_G O^=\text{Al}^{3+}(\text{t})$, and brucitic aluminum $\Delta_G O^=\text{Al}^{3+}(\text{b})$ are unequal in clinocllore, $(\text{Mg}_{2.5}\text{Al}_{0.5})(\text{Si}_3\text{Al})\text{O}_{10}(\text{OH})_2 \cdot (\text{Mg}_{2.5}\text{Al}_{0.5})(\text{OH})_6$ because of the nature of the oxygens surrounding the cations. In the octahedral sites of micas and chlorites, the octahedra comprise four oxygens and two hydroxyls

Table 1. General equation of Gibbs free energy of formation from the oxides of a clinocllore (Mg_{2.5}Al_{0.5})(Si₃Al)O₁₀(OH)₂(Mg_{2.5}Al_{0.5})(OH)₆.

$$\Delta G_{\text{ox}}^{\circ} = -18 \left\{ \begin{aligned} & \frac{2.5}{18} \times \frac{0.75}{18} [\Delta_G O^{\circ} = \text{Mg}^{2+}(\text{o}) - \Delta_G O^{\circ} = \text{Al}^{3+}(\text{o})] + \frac{2.5}{18} \times \frac{6}{18} [\Delta_G O^{\circ} = \text{Mg}^{2+}(\text{o}) - \Delta_G O^{\circ} = \text{Si}^{4+}(\text{t})] \\ & + \frac{2.5}{18} \times \frac{1.5}{18} [\Delta_G O^{\circ} = \text{Mg}^{2+}(\text{o}) - \Delta_G O^{\circ} = \text{Al}^{3+}(\text{t})] + \frac{0.75}{18} \times \frac{6}{18} [\Delta_G O^{\circ} = \text{Al}^{3+}(\text{o}) - \Delta_G O^{\circ} = \text{Si}^{4+}(\text{t})] \\ & + \frac{0.75}{18} \times \frac{1.5}{18} [\Delta_G O^{\circ} = \text{Al}^{3+}(\text{o}) - \Delta_G O^{\circ} = \text{Al}^{3+}(\text{t})] + \frac{2.5}{18} \times \frac{1}{18} [\Delta_G O^{\circ} = \text{Mg}^{2+}(\text{o}) - \Delta_G O^{\circ} = \text{H}^{+}(\text{i})] \\ & + \frac{0.75}{18} \times \frac{1}{18} [\Delta_G O^{\circ} = \text{Al}^{3+}(\text{o}) - \Delta_G O^{\circ} = \text{H}^{+}(\text{i})] + \frac{6}{18} \times \frac{1.5}{18} [\Delta_G O^{\circ} = \text{Si}^{4+}(\text{o}) - \Delta_G O^{\circ} = \text{Al}^{3+}(\text{t})] \\ & + \frac{2.5}{18} \times \frac{0.75}{18} [\Delta_G O^{\circ} = \text{Mg}^{2+}(\text{b}) - \Delta_G O^{\circ} = \text{Al}^{3+}(\text{b})] + \frac{2.5}{18} \times \frac{3}{18} [\Delta_G O^{\circ} = \text{Mg}^{2+}(\text{b}) - \Delta_G O^{\circ} = \text{H}^{+}(\text{b})] \\ & + \frac{0.75}{18} \times \frac{3}{18} [\Delta_G O^{\circ} = \text{Al}^{3+}(\text{b}) - \Delta_G O^{\circ} = \text{H}^{+}(\text{b})] + \frac{6}{18} \times \frac{3}{18} [\Delta_G O^{\circ} = \text{Si}^{4+}(\text{t}) - \Delta_G O^{\circ} = \text{H}^{+}(\text{b})] \\ & + \frac{1.5}{18} \times \frac{3}{18} [\Delta_G O^{\circ} = \text{Al}^{3+}(\text{t}) - \Delta_G O^{\circ} = \text{H}^{+}(\text{b})] \end{aligned} \right\}$$

like $MO_4(OH)_2$; in brucitic sites of chlorites, the octahedra are surrounded by six hydroxyls, probably $M(OH)_6$.

In the general equation, the interaction energy is defined by the difference $\Delta_G O^{\circ} = M_i^{z+}(\text{clay}) - \Delta_G O^{\circ} = M_j^{z+}(\text{clay})$, and this term characterizes short-range interactions between the different sites. The interaction energy is positive (absolute value) and should be assumed to be equal (Vieillard and Tardy, 1988b, 1989):

$$[\Delta_G O^{\circ} = M_i^{z+}(\text{clay}) - \Delta_G O^{\circ} = M_j^{z+}(\text{clay})] = 96.483(\chi_{M_i} - \chi_{M_j})^2 \quad (6)$$

where $\chi_{M^{z+}}$ is Pauling's electronegativity of the cation M^{z+} (Pauling, 1960).

Vieillard (1994a, 2000) applied the principles of Pauling (1960), regarding the predominance of nearest-neighbor interactions (short-range interactions) observed in a crystal structure in the calculation of enthalpy of formation or Gibbs free energy of formation.

In the two kinds of minerals, micas (10 Å) and chlorites (14 Å), the idealized crystal structure is given and shows for each case the existence of common O and non-common O between two consecutive sites (Figure 1).

Thus, for the muscovite, $K(Al_2)(Si_3Al)O_{10}(OH)_2$, where K occupies the interlayer site (labeled l), Al is located in the octahedral site (labeled o), and the tetrahedral site contains Si and Al (labeled t) and proton $H^+(i)$ bonded to oxygens of octahedral sheets. The

method of calculating the Gibbs free energy of formation from constituent oxides is described in Vieillard (2000).

In clinocllore, $(Mg_{2.5}Al_{0.5})(Si_3Al)O_{10}(OH)_2 \cdot (Mg_{2.5}Al_{0.5})(OH)_6$, where octahedral cations Mg^{2+} and Al^{3+} are randomly distributed both in octahedral sites ($MO_4(OH)_2$) and brucitic sites ($M(OH)_6$), there are eight ions located as follows: Mg^{2+} and Al^{3+} in the octahedral site labeled (o); Al^{3+} and Si^{4+} , located in the tetrahedral site labeled (t); Mg^{2+} and Al^{3+} in the brucitic site labeled (b); the proton H^+ occupies two different positions: the first, termed $H^+(i)$, is bonded to oxygen in the octahedral sheet, and the second, $H^+(b)$, bonded to oxygens of the brucitic sheet and oriented towards tetrahedral sheets. In this case, one assumes that the electronegativities of cations located in octahedral sites are the same as those for 10 Å minerals; this explains why the label (o) remains unchanged. By considering the chlorite mineral as a sum of oxides: $(Mg_{2.5}Al_{0.5})(Si_3Al)O_{10}(OH)_2 \cdot (Mg_{2.5}Al_{0.5})(OH)_6 \rightarrow 2.5 MgO(o) + 1/4 Al_2O_3(o) + 3 SiO_2(t) + 0.5 Al_2O_3(t) + H_2O(i) + 2.5 MgO(b) + 1/4 Al_2O_3(b) + 3 H_2O(b)$ with the molar fraction of oxygen bound to the following oxides: $MgO(o)$, $Al_2O_3(o)$, $SiO_2(t)$, $Al_2O_3(t)$, $H_2O(i)$, $MgO(b)$, $Al_2O_3(b)$, and $H_2O(b)$ being, 2.5/18, 0.75/18, 6/18, 1.5/18, 1/18, 2.5/18, 0.75/18, and 3/18, respectively; the calculated equation of $\Delta G_{\text{ox}}^{\circ}$, based on short-range interactions, is given in Table 2. The crystal structure of a chlorite-type mineral (Figure 1) shows the existence of non-common oxygen between the following consecutive cations: $Mg^{2+}(o)$ and

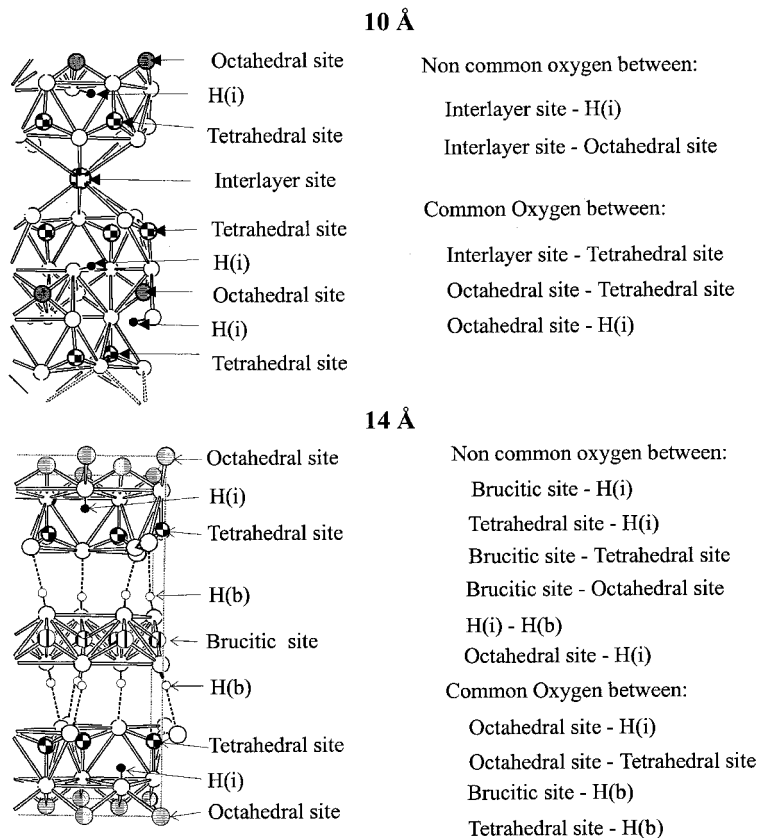


Figure 1. Crystal structures of 10 Å and 14 Å phyllosilicates showing the positions of oxygen atoms between consecutive sites.

$H^+(b)$, $Al^{3+}(o)$ and $H^+(b)$, $Mg^{2+}(b)$ and $H^+(i)$, $Al^{3+}(b)$ and $H^+(i)$, $Si^{4+}(t)$ and $H^+(i)$, $Al^{3+}(t)$ and $H^+(i)$, $Si^{4+}(t)$ and $Mg^{2+}(b)$, $Si^{4+}(t)$ and $Al^{3+}(b)$, $Al^{3+}(t)$ and $Mg^{2+}(b)$, $Al^{3+}(t)$ and $Al^{3+}(b)$, $Mg^{2+}(o)$ and $Mg^{2+}(b)$, $Mg^{2+}(o)$ and $Al^{3+}(b)$, $Al^{3+}(o)$ and $Mg^{2+}(b)$, $Al^{3+}(o)$ and $Al^{3+}(b)$, and finally $H^+(i)$ and $H^+(b)$. This means that long-range interaction energy terms between two sites (*i.e.* 15 interaction energy terms between the sites listed), $[\Delta_G O^=M_i^{z_i+}(\text{clay}) - \Delta_G O^=M_j^{z_j+}(\text{clay})]$ are equal to zero and did not appear in the general equation of ΔG_{ox}^0 (Table 1).

RESULTS

Thermodynamic set of data for clay minerals

The numerous data for Gibbs free energies of formation of micas and chlorites are compiled elsewhere (Chatterjee *et al.*, 1998; Robie and Hemingway, 1995; Johnson *et al.*, 1992; Holland and Powell, 1990; Wolery and Daveler, 1992) and many of them are inconsistent. To provide an internally consistent set of data, the solubility product of each clay mineral is first calculated from internal data (same references for both clay minerals and ions), then Gibbs free energies for each

clay mineral are calculated again from the calculated solubility product with the new set of thermodynamic data of ions (Table 2). A few experimental solubility products of some chlorites are used (Kittrick, 1982). Gibbs free energies of 44 dehydrated end-member, well-crystallized phyllosilicates from Tardy and Duplay (1992) were recalculated from the estimated solubility products with ΔG_f^0 of ions (Table 2). These values were used here to determine the importance of the interlayer cations in different clay minerals.

Minimization

Firstly, parameter $\Delta_G O^=M^{z+}$ of eleven cations characterizing the occurrence in different sites (Na^+ , K^+ , Ca^{2+} and Mg^{2+} in the interlayer site, Mg^{2+} , Fe^{2+} , Al^{3+} and Fe^{3+} in octahedral sites, Si^{4+} and Al^{3+} in tetrahedral sites and H^+ in the hydroxyl) of the 10 Å minerals were determined by minimizing the difference between calculated Gibbs free energies of formation from oxides and those computed by the general equation 2. Constraints of minimization involve short-range interactions and positive value terms of interaction energies between two different cations in accordance with equation 6.

Table 2. Gibbs free energies of formation of oxides and ions at 298.15 K and calculated parameter $\Delta_G O^{\ominus} M^{z+}(\text{aq})$ of selected cations.

Oxides	ΔG_f° , 298.15 K (kJ mol ⁻¹)	Ions	ΔG_f° , 298.15 K (kJ mol ⁻¹)	$\Delta_G O^{\ominus} M^{z+}(\text{aq})$ (kJ mol ⁻¹)
Li ₂ O	-561.2 ¹	Li ⁺	-292.6 ⁷	24.00
Na ₂ O	-376.0 ¹	Na ⁺	-261.881 ⁷	147.76
K ₂ O	-322.1 ¹	K ⁺	-282.462 ⁷	242.82
Cs ₂ O	-308.4 ¹	Cs ⁺	-291.46 ³	274.52
(NH ₄) ₂ O	-234.3 ²	NH ₄ ⁺	-79.414 ³	-75.47
BaO	-520.4 ¹	Ba ²⁺	-563.8 ⁷	43.40
CaO	-603.1 ¹	Ca ²⁺	-552.79 ⁷	-50.31
MgO	-569.3 ¹	Mg ²⁺	-453.985 ⁷	-115.32
BeO	-580.10 ²	Be ²⁺	-378.86 ⁸	-201.24
FeO	-251.4 ¹	Fe ²⁺	-90.53 ⁹	-160.87
MnO	-362.9 ¹	Mn ²⁺	-228.1 ¹	-134.80
CuO	-128.3 ¹	Cu ²⁺	65.1 ¹	-193.40
CoO	-214.1 ¹	Co ²⁺	-54.392 ⁷	-159.71
NiO	-211.1 ¹	Ni ²⁺	-45.6 ⁷	-165.50
CdO	-258.35 ³	Cd ²⁺	-77.6 ¹	-151.1
ZnO	-320.4 ¹	Zn ²⁺	-147.3 ¹	-173.10
Fe ₂ O ₃	-744.4 ¹	Fe ³⁺	-16.28 ⁹	-237.28
Cr ₂ O ₃	-1053.1 ¹	Cr ³⁺	-206.27 ⁸	-213.52
Al ₂ O ₃	-1582.3 ¹	Al ³⁺	-487.616 ¹⁰	-202.36
Ga ₂ O ₃	-998.4 ⁴	Ga ³⁺	-158.992 ⁷	-226.78
SiO ₂	-856.3 ⁴	SiO _{2(aq)} ^o	-833.411 ⁷	
TiO ₂	-888.8 ¹	Ti ⁴⁺	-386.34 ¹¹	-251.2
H ₂ O (i)	-220.0 ⁵	H ₂ O liq.	-237.183 ⁷	
H ₂ O (b)	-228.0 ⁶			
H ₂ O (e)	-210.0 ⁶			

¹ Robie and Hemingway (1995); ² Wilcox and Bromley (1963); ³ Codata (1989); ⁴ Barin (1985); ⁵ Vieillard (2000); ⁶ this work; ⁷ Shock and Helgeson (1988); ⁸ Sverjensky *et al.* (1997); ⁹ Parker and Khodakovskii (1995); ¹⁰ Pokrovskii and Helgeson (1995);

¹¹ Calculated from ΔH_f° of Vasil'ev *et al.* (1986) and S° of Shock and Helgeson (1988).

The minimization is optimized by fixing $\Delta G_f^{\circ} \text{H}_2\text{O}(\text{i})$ at $-220.0 \text{ kJ mol}^{-1}$, with a value slightly different from those of ice II, $\Delta G_f^{\circ} = -235.56 \text{ kJ mol}^{-1}$ (Mercury *et al.*, 2001) and identical to those found by Vieillard (2000) in the prediction of Gibbs free energies of formation of hydrated clay minerals. This difference is based on the differences between the proton of the hydroxyl groups in the 2:1 layer vs. the proton of ice. By assuming that $\Delta G_f^{\circ} \text{H}^+(\text{c}) = 0$, $\Delta_G O^{\ominus} \text{H}^+(\text{i})$ is equal to $-220.0 \text{ kJ mol}^{-1}$, which represents the reference value for $\Delta_G O^{\ominus} M^{z+}(\text{clay})$ for different cations located in different sites of micas and brittle micas (Table 3).

Secondly, thanks to the new set of $\Delta_G O^{\ominus} M^{z+}(\text{clay})$ obtained for octahedral and tetrahedral sites from micas (Table 3), the determination of $\Delta_G O^{\ominus} M^{z+}$ for the five cations (Li⁺, Mg²⁺, Fe²⁺, Al³⁺, and Fe³⁺) in the brucitic site and $\Delta_G O^{\ominus} \text{H}^+(\text{b})$ is now performed by minimizing the difference between experimental and calculated Gibbs free energies of formation from the oxides of chlorites, with the same constraints as given below. Gibbs free energies of formation of clinocllore, chamosite, cookeite, sudoite, ripidolite and four natural clinocllore for which solubility data are available (Kittrick, 1982), were recalculated with the new set of

Gibbs free energies of formation of ions to maintain an internally consistent set of data (Table 4).

The minimization is optimized by fixing $\Delta G_f^{\circ} \text{H}_2\text{O}(\text{b}) = \Delta_G O^{\ominus} \text{H}^+(\text{b})$ at $-228.0 \text{ kJ mol}^{-1}$, a value slightly more negative than those obtained for the hydroxyl group in the 2:1 layers. This slight difference probably explains why the protons of the brucitic sheet oriented towards oxygens of tetrahedral sheets are more tightly bonded than those of hydroxyl in the 2:1 layers for which protons are oriented depending on the nature of cations in octahedral sites. Two natural Fe-bearing chlorites from Ishpeming (Michigan) and New Mexico were discarded in the processing of minimization because of the uncertainties about their solubility products and the non-reversibility between fluid compositions and starting solid phases (Aja and Small, 1999). The new set of values of $\Delta_G O^{\ominus} M^{z+}(\text{clay})$ in different sites (interlayer, octahedral, brucitic and tetrahedral) obtained by minimization are given in Table 4 and they contribute to the determination of Gibbs free energy of formation from constituent oxides. Consequently the determined Gibbs free energies of formation of the 10 Å and 14 Å minerals may be compared with experimental (or calculated) values and are given in Table 4.

Table 3. Values of parameter $\Delta_G O^{\ominus} M^{z+}(\text{clay})$ for different ions located in different sites (interlayer, tetrahedral, octahedral and brucitic sites) obtained by minimization or calculated from equations 8 to 11.

Ions (interlayer)	$\Delta_G O^{\ominus} M^{z+}(\text{aq})$ (kJ mol ⁻¹)	$\Delta_G O^{\ominus} M^{z+}(\text{l})$ (kJ mol ⁻¹)	Ions (tetrahedral)	$\Delta_G O^{\ominus} M^{z+}(\text{aq})$ (kJ mol ⁻¹)	$\Delta_G O^{\ominus} M^{z+}(\text{t})$ (kJ mol ⁻¹)
K ⁺ (l)		476 ¹	Si ⁴ (t)		-169 ¹
Na ⁺ (l)		280 ¹	Al ³⁺ (t)		-196 ¹
Ca ²⁺ (l)		-52 ¹	Fe ³⁺ (t)	-237.28	-261.7 ⁵
Mg ²⁺ (l)		-110 ¹	Ga ³⁺ (t)	-226.79	-241.9 ⁵
Cs ⁺ (l)	274.52	562.1 ³	Be ²⁺ (t)	-201.24	-193.9 ⁵
Rb ⁺ (l)	267.96	545.1 ³			
Ba ²⁺ (l)	40.382	73.7 ³			
Sr ²⁺ (l)	3.140	18.8 ³			
NH ₄ ⁺ (l)	-75.47	-76.6 ³			
Fe ²⁺ (l)	-160.87	-148.7 ³			

Ions (octahedral)	$\Delta_G O^{\ominus} M^{z+}(\text{aq})$ (kJ mol ⁻¹)	$\Delta_G O^{\ominus} M^{z+}(\text{o})$ (kJ mol ⁻¹)	Ions (brucitic)	$\Delta_G O^{\ominus} M^{z+}(\text{aq})$ (kJ mol ⁻¹)	$\Delta_G O^{\ominus} M^{z+}(\text{b})$ (kJ mol ⁻¹)
Mg ²⁺ (o)		-103 ¹	Mg ²⁺ (b)		-30 ²
Fe ²⁺ (o)		-141 ¹	Fe ²⁺ (b)		-115 ²
Al ³⁺ (o)		-157 ¹	Al ³⁺ (b)		-171 ²
Fe ³⁺ (o)		-168.5 ¹	Fe ³⁺ (b)		-210 ²
Li ⁺ (o)	24.00	-35.2 ¹	Li ⁺ (b)		70 ²
Mn ²⁺ (o)	-134.80	-119.1 ⁴	Mn ²⁺ (b)	-134.80	-87.3 ⁶
Zn ²⁺ (o)	-173.10	-139.3 ⁴	Zn ²⁺ (b)	-173.10	-129.1 ⁶
Ni ²⁺ (o)	-165.50	-135.3 ⁴	Ni ²⁺ (b)	-165.50	-120.8 ⁶
Co ²⁺ (o)	-159.71	-132.2 ⁴	Co ²⁺ (b)	-159.71	-114.5 ⁶
Cr ³⁺ (o)	-213.52	-160.6 ⁴	Cr ³⁺ (b)	-213.52	-173.1 ⁶
Ca ²⁺ (o)	-50.31	-74.4 ⁴	Ca ²⁺ (b)	-50.31	4.7 ⁶
Ga ³⁺ (o)	-226.79	-167.6 ⁴			
Ti ⁴⁺ (o)	-246.73	-180.5 ⁴			
H ⁺ (i)		-220 ¹	H ⁺ (b)		-228 ²

¹ Obtained by minimization of the difference between calculated $\Delta G_{\text{ox}, 298.15\text{K}}^{\circ}$ and measured $\Delta G_{\text{ox}, 298.15\text{K}}^{\circ}$ for micas; ² obtained by minimization of the difference between calculated

$\Delta G_{\text{ox}, 298.15\text{K}}^{\circ}$ and measured $\Delta G_{\text{ox}, 298.15\text{K}}^{\circ}$ for chlorites; ³ calculated from equation 8;

⁴ calculated from equation 9; ⁵ calculated from equation 10; ⁶ see text.

Precision of the method of prediction

Figure 2 compares this method with other methods of predicted values (Nriagu, 1975; Chermak and Rimstidt, 1989). It shows a plot of standard errors of estimation using our model and the average error obtained for each of the two different methods given previously. The horizontal and vertical dashed lines show the $\pm 0.25\%$ error for each model. The data from clay minerals arranged in nine groups: pyrophyllite, true micas (muscovite, paragonite, annite, phlogopite), celadonite, brittle micas (siderophyllite, eastonite, margarite), Mg-chlorites, Fe-chlorites, natural chlorites (Kittrick, 1982), aluminous chlorites and other chlorite minerals (ripidolite, sudoite, cookeite), for use in determining the accuracy of prediction.

It appears that these two methods (Nriagu, 1975; Chermak and Rimstidt, 1989) give predicted Gibbs free energies of formation with a very large uncertainty; this

is due to the fact that these methods are built on an additive scheme and do not take into account the interaction energies between cations in the same layer. In both Figures 2a and b, the ferrous chlorites (Ishpeming and New Mexico) shown by two points very far from the group, exhibit an abnormal Gibbs free energy of formation. The method of Nriagu (1975) (Figure 2a) provides predicted Gibbs free energies of formation which are systematically less negative than the experimental values ($>0.5\%$) except for pyrophyllite, talc-brucite and aluminous chlorites.

The method of Chermak and Rimstidt (1989) (Figure 2b) initially tested on silicate minerals, gives an accuracy within a 0.5% limit for 10 Å phyllosilicates such as muscovite, phlogopite and talc. For celadonites and brittle micas, the error reaches $\pm 1\%$; and nearly all the values of Gibbs free energy of formation from elements of chlorites are overestimated ($>0.8\%$).

Table 4. Chemical composition, listed Gibbs free energies of formation, calculated solubility products, calculated and predicted Gibbs free energies of formation at 298.15 K of pyrophyllites, micas, celadonites, brittle micas and chlorites.

Mineral	Formula	ΔG_f° , 298.15 K listed (kJ mol ⁻¹)	Log K	ΔG_f° , 298.15 K calculated (kJ mol ⁻¹)	ΔG_f° , 298.15 K predicted (kJ mol ⁻¹)	Error (%)
Pyrophyllite group						
Pyrophyllite ¹	(Al ₂)(Si ₄)O ₁₀ (OH) ₂	-5266.20	-1.04	-5263.57	-5267.25	-0.07
Minnesotaite ²	(Fe ₃)(Si ₄)O ₁₀ (OH) ₂	-4477.08	13.03	-4479.61	-4475.15	0.10
Talc ¹	(Mg ₃)(Si ₄)O ₁₀ (OH) ₂	-5520.20	22.33	-5516.89	-5514.35	0.05
Talc ³	(Mg ₃)(Si ₄)O ₁₀ (OH) ₂	-5515.37	23.17	-5512.06	-5514.35	-0.04
Talc ⁴	(Mg ₃)(Si ₄)O ₁₀ (OH) ₂	-5515.57	23.14	-5512.26	-5514.35	-0.04
Mica group						
Muscovite ¹	(K)(Al ₂)(Si ₃ Al)O ₁₀ (OH) ₂	-5608.40	11.35	-5603.84	-5595.28	0.15
Muscovite ³	(K)(Al ₂)(Si ₃ Al)O ₁₀ (OH) ₂	-5600.41	12.75	-5595.85	-5595.28	0.01
Muscovite ⁴	(K)(Al ₂)(Si ₃ Al)O ₁₀ (OH) ₂	-5602.19	12.44	-5597.63	-5595.28	0.04
Annite ¹	(K)(Fe ₃ ²⁺)(Si ₃ Al)O ₁₀ (OH) ₂	-4798.30	29.10	-4798.90	-4801.18	-0.05
Annite ⁴	(K)(Fe ₃ ²⁺)(Si ₃ Al)O ₁₀ (OH) ₂	-4793.88	29.87	-4794.48	-4801.18	-0.14
Phlogopite ¹	(K)(Mg ₃)(Si ₃ Al)O ₁₀ (OH) ₂	-5860.50	35.06	-5855.26	-5835.63	0.34
Phlogopite ³	(K)(Mg ₃)(Si ₃ Al)O ₁₀ (OH) ₂	-5828.93	40.59	-5823.69	-5835.63	-0.20
Phlogopite ⁴	(K)(Mg ₃)(Si ₃ Al)O ₁₀ (OH) ₂	-5833.59	39.77	-5828.35	-5835.63	-0.12
Paragonite ¹	(Na)(Al ₂)(Si ₃ Al)O ₁₀ (OH) ₂	-5568.50	14.66	-5564.36	-5560.98	0.06
Paragonite ³	(Na)(Al ₂)(Si ₃ Al)O ₁₀ (OH) ₂	-5567.05	14.92	-5562.91	-5560.98	0.03
Paragonite ⁴	(Na)(Al ₂)(Si ₃ Al)O ₁₀ (OH) ₂	-5562.77	15.67	-5558.63	-5560.98	-0.04
Tschermak Talc-Mg ³	(Mg _{0.5})(Mg _{1.5} Al)(Si ₃ Al)O ₁₀ (OH) ₂	-5613.92	34.72	-5608.35	-5666.05	-1.03
Rectorite ⁵	(Na _{0.67})(Al ₂)(Si _{3.33} Al _{0.67})O ₁₀ (OH) ₂	-5471.44	8.80	-5467.80	-5466.37	0.03
Celadonite group						
Celadonite Al-Mg ⁶	(K)(MgAl)(Si ₄)O ₁₀ (OH) ₂	-5463.86	7.86	-5461.56	-5462.08	-0.01
Celadonite Al-Mg ³	(K)(MgAl)(Si ₄)O ₁₀ (OH) ₂	-5456.97	9.07	-5454.67	-5462.08	-0.14
Celadonite Al-Fe ³	(K)(Fe ²⁺ Al)(Si ₄)O ₁₀ (OH) ₂	-5118.56	4.34	-5118.20	-5110.93	0.14
Brittle mica group						
Siderophyllite ³	(K)(Fe ₂ ²⁺ Al)(Si ₂ Al ₂)O ₁₀ (OH) ₂	-5262.15	40.66	-5258.54	-5280.23	-0.41
Eastonite ³	(K)(Mg ₂ Al)(Si ₂ Al ₂)O ₁₀ (OH) ₂	-5949.22	48.33	-5941.72	-5976.20	-0.58
Eastonite ⁷	(K)(Mg ₂ Al)(Si ₂ Al ₂)O ₁₀ (OH) ₂	-5976.38	43.57	-5968.88	-5976.20	-0.12
Margarite ¹	(Ca)(Al ₂)(Si ₂ Al ₂)O ₁₀ (OH) ₂	-5858.90	37.82	-5851.68	-5859.30	-0.13
Margarite ³	(Ca)(Al ₂)(Si ₂ Al ₂)O ₁₀ (OH) ₂	-5857.32	38.09	-5850.10	-5859.30	-0.16
Margarite ⁴	(Ca)(Al ₂)(Si ₂ Al ₂)O ₁₀ (OH) ₂	-5857.16	38.12	-5849.94	-5859.30	-0.16
Mg-chlorites						
Amesite 14 Å ²	(Mg ₄ Al ₂)(Si ₂ Al ₂)O ₁₀ (OH) ₈	-8323.06	75.46	-8323.06	-8336.82	-0.17
Amesite 14 Å ⁸	(Mg ₄ Al ₂)(Si ₂ Al ₂)O ₁₀ (OH) ₈	-8350.84	72.66	-8339.02	-8336.82	0.03
Clinochlore ¹	(Mg ₅ Al)(Si ₃ Al)O ₁₀ (OH) ₈	-8255.80	60.50	-8246.24	-8190.83	0.67
Clinochlore ³	(Mg ₅ Al)(Si ₃ Al)O ₁₀ (OH) ₈	-8256.03	60.46	-8246.46	-8190.83	0.67
Clinochlore ²	(Mg ₅ Al)(Si ₃ Al)O ₁₀ (OH) ₈	-8207.77	68.92	-8198.20	-8190.83	0.09
Talc 3 brucite ⁸	(Mg ₆)(Si ₄)O ₁₀ (OH) ₈	-8065.46	65.04	-8058.16	-8030.17	0.35
Fe-chlorites						
Chamosite 14 Å ³	(Fe ₅ ²⁺ Al)(Si ₃ Al)O ₁₀ (OH) ₈	-6541.71	40.72	-6541.87	-6508.23	0.51
Chamosite 14 Å ⁹	(Fe ₅ ²⁺ Al)(Si ₃ Al)O ₁₀ (OH) ₈	-6495.13	48.88	-6495.29	-6508.23	-0.20
Natural chlorites						
Chlorite Vermont ^{10,11}		-7793.00	53.82	-7798.12	-7791.15	0.09
Chlorite Ishpeming ^{10,12}		-7290.00	24.64	-7322.04	-7153.95	2.30
Chlorite Québec ^{10,13}		-7869.00	52.40	-7870.87	-7859.09	0.15
Chlorite New Mexico ^{10,14}		-7319.00	22.73	-7344.53	-7220.60	1.69
Aluminous chlorites						
Chlorite alumineuse ¹⁵	(Al ₄)(Si _{3.4} Al _{0.6})O ₁₀ (OH) ₈	-7709.83	22.46	-7702.39	-7755.09	-0.68
Dombassite ¹⁶	(Al ₄)(Si ₄)O ₁₀ (OH) ₈	-7573.40	15.50	-7567.45	-7627.47	-0.79
Other chlorites						
Ripidolite ⁶	(Mg ₃ Fe ₂ ²⁺ Al)(Si ₃ Al)O ₁₀ (OH) ₈	-7518.62	61.62	-7512.95	-7528.04	-0.20
Sudoite ¹⁷	(Mg ₂ Al ₃)(Si ₃ Al)O ₁₀ (OH) ₈	-7985.56	39.98	-7976.68	-7995.79	-0.24
Sudoite ¹⁸	(Mg ₂ Al ₃)(Si ₃ Al)O ₁₀ (OH) ₈	-7984.84	40.10	-7975.96	-7995.79	-0.25
Cookeite ⁴	(Al ₄ Li)(Si ₃ Al)O ₁₀ (OH) ₈	-7882.79	35.47	-7874.65	-7895.42	-0.16

¹ Robie and Hemingway (1995); ² Johnson *et al.* (1992); ³ Holland and Powell (1990); ⁴ Chatterjee *et al.* (1998); ⁵ Vidal (1997); ⁶ Wolery and Daveler (1992); ⁷ Zolotov *et al.* (1999); ⁸ McPhail *et al.* (1990); ⁹ Saccocia and Seyfried (1993); ¹⁰ Kittrick (1982); ¹¹ (Mg_{3.24}Fe_{0.99}Al_{1.45}Fe_{0.07}³⁺)(Si_{2.98}Al_{1.02})O₁₀(OH)₈; ¹² (Mg_{1.05}Fe_{3.3}Al_{1.61})(Si_{2.47}Al_{1.53})O₁₀(OH)₈; ¹³ (Mg_{3.53}Fe_{0.58}Al_{1.39}Fe_{0.21}³⁺)(Si_{2.99}Al_{1.01})O₁₀(OH)₈; ¹⁴ (Mg_{1.16}Fe_{2.61}Al_{1.75}Fe_{0.12}³⁺)(Si_{2.84}Al_{1.16})O₁₀(OH)₈; ¹⁵ Varadachari *et al.* (1994); ¹⁶ Merceron *et al.* (1992); ¹⁷ Vidal *et al.* (1992); ¹⁸ El-Din and El-Shazly (1996).

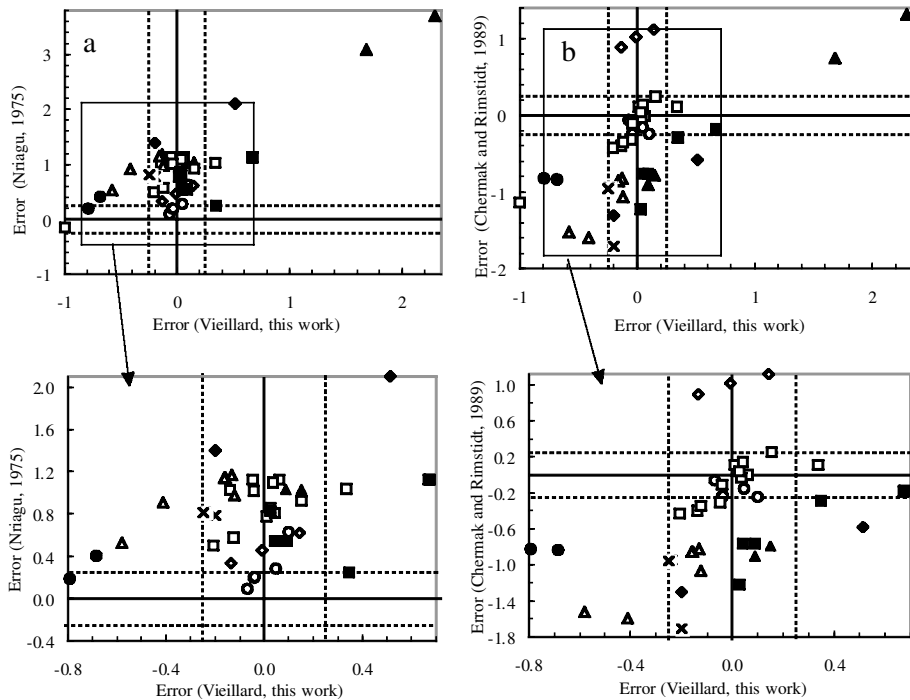


Figure 2. Plots of the percentage errors from different methods of prediction of Gibbs free energies of formation against the percentage errors for values from the model presented here. The horizontal and vertical dashed lines represent a $\pm 0.25\%$ error using in each model: (a) the method of Nriagu (1975); (b) the method of Chermak and Rimstidt (1989). \square muscovite group; \circ pyrophyllite group; \diamond celadonites; \triangle brittle micas; \blacksquare Mg-chlorites; \blacklozenge Fe-chlorites; \bullet aluminous chlorites; \blacktriangle natural chlorites (Kittrick, 1982); \times other chlorites (sudoite, ripidolite, cookeite).

RESULTS

Values of $\Delta_G O^{\bar{M}z^+}(\text{clay})$, obtained from minimization (Table 3) are different from those given for hydrated clays minerals (Vieillard, 2000). Among values of $\Delta_G O^{\bar{M}z^+}(\text{clay})$ corresponding to different sites in the clay mineral, four sets of values were observed corresponding to the interlayer, octahedral, brucitic and tetrahedral sites.

Interlayer sites

The relation between $\Delta_G O^{\bar{M}z^+}(\text{aq})$ and $\Delta_G O^{\bar{M}z^+}(\text{l})$ in the interlayer site for alkaline, earth alkaline cations, (Figure 3a) is:

$$\Delta_G O^{\bar{M}z^+}(\text{l}) = 14.465 + 1.3766[\Delta_G O^{\bar{M}z^+}(\text{aq})] + 0.00225[\Delta_G O^{\bar{M}z^+}(\text{aq})]^2 \quad (8)$$

with a regression coefficient of 0.9994, for five points and a standard error of $\pm 17.4 \text{ kJ mol}^{-1}$. Thus, values of $\Delta_G O^{\bar{M}z^+}(\text{l})$ for NH_4^+ , Ba^{2+} , Sr^{2+} , Rb^+ , Cs^+ located in the interlayer sites can be determined from equation 8 from known values of $\Delta_G O^{\bar{M}z^+}(\text{aq})$ (Table 2) and these values are given in Table 3. By comparing the relationship between $\Delta_G O^{\bar{M}z^+}(\text{aq})$ and $\Delta_G O^{\bar{M}z^+}(\text{l})$ in the interlayer site obtained in hydrated clays (Vieillard, 2000), it appears that the parameter $\Delta_G O^{\bar{M}z^+}(\text{l})$ for interlayer cations in micas is more negative than those observed in hydrated clays minerals except for monovalent cations such as Na^+ , K^+ , Rb^+ and Cs^+ (Figure 3a).

Octahedral sites

A relationship between $\Delta_G O^{\bar{M}z^+}(\text{o})$ and $\Delta_G O^{\bar{M}z^+}(\text{aq})$ is observed for four cations Mg^{2+} , Fe^{2+} , Al^{3+} and Fe^{3+} (Figure 3b):

$$\Delta_G O^{\bar{M}z^+}(\text{o}) = -47.877 + 0.5281[\Delta_G O^{\bar{M}z^+}(\text{aq})] \quad (9)$$

with a regression coefficient of 0.9737 and an error of prediction of $\pm 13.0 \text{ kJ mol}^{-1}$. From equation 9, values of $\Delta_G O^{\bar{M}z^+}(\text{o})$ of cations such as Li^+ , Mn^{2+} , Ni^{2+} , Co^{2+} , Zn^{2+} , Cr^{3+} and Ti^{4+} are determined from known values of $\Delta_G O^{\bar{M}z^+}(\text{aq})$ (Table 2). These values contribute to the prediction of Gibbs free energies of micas and brittle micas with transition metals and Li located in octahedral sites such as lepidolite, ephesite, biotite and transition metals-bearing micas (Table 5).

Brucitic sites

A relationship between $\Delta_G O^{\bar{M}z^+}(\text{b})$ and $\Delta_G O^{\bar{M}z^+}(\text{aq})$ is observed for five cations Li^+ , Mg^{2+} , Fe^{2+} , Al^{3+} and Fe^{3+} (Figure 3b):

$$\Delta_G O^{\bar{M}z^+}(\text{b}) = 59.559 + 1.089[\Delta_G O^{\bar{M}z^+}(\text{aq})] \quad (10)$$

with a regression coefficient of 0.9824 for four points and an error of prediction of $\pm 29.2 \text{ kJ mol}^{-1}$. From equation 10, values of $\Delta_G O^{\bar{M}z^+}(\text{b})$ of cations such as Li^+ , Mn^{2+} , Ni^{2+} , Co^{2+} , Zn^{2+} and Cr^{3+} are determined from known values of $\Delta_G O^{\bar{M}z^+}(\text{aq})$ (Table 2). These values contribute to the prediction of Gibbs free energies

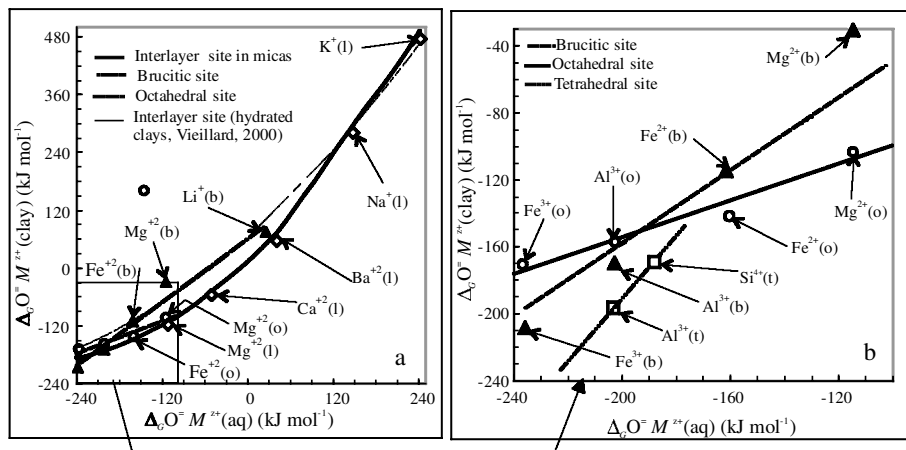


Figure 3. Relationship between $\Delta_G O^=M^{z+}(\text{clay})$ and $\Delta_G O^=M^{z+}(\text{aq})$: (a) for cations in interlayer, brucitic and octahedral positions; (b) for octahedral, brucitic and tetrahedral cations.

of chlorites with transition metals and Li located in brucitic sites such as Co-chlorite, Ni-chlorite and Zn-chlorite (Table 5). It appears that the values of $\Delta_G O^=M^{z+}(\text{b})$ are more negative for trivalent cations than those of the octahedral sheet; for divalent cations the reverse case can be observed.

Tetrahedral sites

The parameter $\Delta_G O^=Al^{3+}(\text{t})$ is more negative than $\Delta_G O^=Si^{4+}(\text{t})$; the difference between the two $\Delta_G O^=$ parameters is always positive with a value of 27.0 kJ mol⁻¹. The prediction of the $\Delta_G O^=M^{z+}(\text{t})$ value of trivalent Fe, Ga and divalent Be in tetrahedral sites is currently possible if one assumes a value of $\Delta_G O^=Si^{4+}(\text{aq})$ equal to -188.0 kJ mol⁻¹ (Tardy and Garrels, 1977; Gartner, 1979). The evaluation of these parameters (Table 3) will allow us to predict Gibbs free energies of formation of some micas such as ferriannite and bityite having Fe³⁺ and Be²⁺ in the tetrahedral site, respectively (Table 5).

Gibbs free energies of formation of some various cations in different sites have been calculated and compared with experimental and estimated values (Table 5). The results appear very good for experimental data (biotite, tobelite, ephesite, ferriannite) and not so good for transition metal-bearing pyrophyllite, micas and chlorites for which Gibbs free energies of formation from elements are estimated by a linear regression from Mg- and Fe²⁺-bearing phyllosilicates (Sverjensky, 1985). His poor choice of the Gibbs free energies of formation of minnesotaite ($\Delta_G^\circ_f = -4390.7$ kJ mol⁻¹) explains the very great underestimation of Gibbs free energies for Co-, Ni-, Zn- and Mn-bearing pyrophyllite. Some Li-rich micas (polyolithionite-OH, trilithionite-OH and lepidolite-OH) for which Gibbs free energies of formation are predicted, can be compared with experimental Gibbs free energies of formation of these F- and Li-rich micas (Ponomareva and Gordienko, 1991).

DISCUSSION

Example of calculation of Gibbs free energies of a chlorite mineral

A low-Fe clinocllore chlorite with the following chemical formula: $(Mg_{4.152}Mn_{0.004}Ca_{0.01}Ni_{0.008}Cr_{0.004}Ti_{0.005}Fe_{0.43}Al_{1.126}Fe_{0.172}^{3+})(Si_{2.875}Al_{1.125})O_{10}(OH)_8$ has its solubility measured experimentally by equilibration in aqueous solutions at 25, 125 and 175°C and saturated vapor pressures (Aja and Small, 1999). Reversibility of fluid mineral equilibria was demonstrated by approaching final solution compositions from different ratios of Mg²⁺ and under- and super- saturation of silica. By assuming a random distribution of cations in octahedral and brucitic sites, and with the help of $\Delta_G O^=M^{z+}(\text{clay})$ (Tables 4) and equation 2, the Gibbs free energy of formation from constituent oxides can be computed and is $\Delta_G O_{ox}^\circ = -278.2$ kJ mol⁻¹. Thanks to the values of Gibbs free energies of formation of the constituent oxides (Table 1), the Gibbs free energy of formation from elements is $\Delta_G^\circ_f = -7974.8$ kJ mol⁻¹. This predicted value is very close to those calculated from equation 1 in Aja and Small (1999); $\Delta_G^\circ_f = -7953.51$ kJ mol⁻¹ computed from $\Delta_G^\circ_f(\text{kaolinite}) = -3797.5$ kJ mol⁻¹ (Robie and Hemingway, 1995); $\Delta_G^\circ_f Al(OH)_4^-(\text{aq}) = -1306.077$ kJ mol⁻¹ (Diakonov *et al.*, 1996) and $\Delta_G^\circ_f Fe(OH)_4^-(\text{aq}) = -842.558$ kJ mol⁻¹ (Baes and Mesmer, 1976).

Non-constancy of the $\Delta_G O^=M^{z+}$ parameter

By assuming the constancy of the parameter $\Delta_G O^=M^{z+}(\text{clay})$ within three sites of a clay mineral (tetrahedral, octahedral and brucitic), this work shows that this model of prediction of Gibbs free energies of formation from oxides can give very good results if the formalism of the Gibbs free energy of formation from constituent oxides uses an approach from short-range interactions. The assumption of the constancy of the

Table 5. Chemical composition, experimental or calculated solubility products, calculated and predicted Gibbs free energies of formation from elements at 298.15 K of transition elements bearing phyllosilicates.

Sample	Formula	Log K	ΔG_f° , 298.15 K calculated (kJ mol ⁻¹)	ΔG_f° , 298.15 K predicted (kJ mol ⁻¹)	Error (%)
Biotite-Mg ¹	(K)(Mg _{2.17} Al _{0.42} Ti _{0.18})(Si _{2.69} Al _{1.31})O ₁₀ (OH) ₂	23.66	-5806.43	-5809.35	-0.05
Biotite-Fe ¹	(K)(Fe _{2.17} Al _{0.42} Ti _{0.18})(Si _{2.69} Al _{1.31})O ₁₀ (OH) ₂	12.82	-5079.62	-5060.37	0.38
Tobelite ²	(NH ₄)(Al ₂)(Si ₃ Al)O ₁₀ (OH) ₂	0.56	-5383.00	-5378.69	0.08
Tschermak Talc-Fe ³	(Fe _{0.5})(Fe _{1.5} Al)(Si ₃ Al)O ₁₀ (OH) ₂	28.47	-4917.09	-4970.67	-1.09
Ephesite ⁴	(Na)(LiAl ₂)(Si ₂ Al ₂)O ₁₀ (OH) ₂	36.59	-5860.35	-5849.45	0.19
Pyrophyllite-Ga ⁵	(K)(Ga ₂)(Si ₃ Al)O ₁₀ (OH) ₂	-8.32	-4647.86	-4653.89	-0.13
Ferriannite ⁶	(K)(Fe ₃ ²⁺)(Si ₃ Fe ³⁺)O ₁₀ (OH) ₂	11.07	-4430.47	-4460.22	-0.67
Talc-Mn ⁷	(Mn ₃)(Si ₄)O ₁₀ (OH) ₂		-4816.62	-4860.84	-0.92
Talc-Co ⁷	(Co ₃)(Si ₄)O ₁₀ (OH) ₂		-4272.70	-4383.02	-2.58
Talc-Ni ⁷	(Ni ₃)(Si ₄)O ₁₀ (OH) ₂		-4255.96	-4367.14	-2.61
Talc-Zn ⁷	(Zn ₃)(Si ₄)O ₁₀ (OH) ₂		-4566.42	-4686.01	-2.62
Muscovite-Mn ⁷	(K)(Mn ₃)(Si ₃ Al)O ₁₀ (OH) ₂		-5191.51	-5184.02	0.14
Muscovite-Co ⁷	(K)(Co ₃)(Si ₃ Al)O ₁₀ (OH) ₂		-4691.50	-4707.95	-0.35
Muscovite-Ni ⁷	(K)(Ni ₃)(Si ₃ Al)O ₁₀ (OH) ₂		-4676.46	-4692.45	-0.34
Muscovite-Zn ⁷	(K)(Zn ₃)(Si ₃ Al)O ₁₀ (OH) ₂		-4961.80	-5011.82	-1.01
Chlorite-Mn ⁷	(Mn ₅ Al)(Si ₃ Al)O ₁₀ (OH) ₈ 14 Å		-7133.72	-7106.5	0.38
Chlorite-Co ⁷	(Co ₅ Al)(Si ₃ Al)O ₁₀ (OH) ₈ 14 Å		-6307.38	-6333.5	-0.41
Chlorite-Ni ⁷	(Ni ₅ Al)(Si ₃ Al)O ₁₀ (OH) ₈ 14 Å		-6282.28	-6311.1	-0.46
Chlorite-Zn ⁷	(Zn ₅ Al)(Si ₃ Al)O ₁₀ (OH) ₈ 14 Å		-6753.81	-6848.1	-1.40
Polyolithonite ⁸	(K)(Li ₂ Al)(Si ₄)O ₁₀ (OH) ₂			-5513.3	
Trilithionite ⁸	(K)(Li _{1.5} Al _{1.5})(Si ₃ Al)O ₁₀ (OH) ₂			-5702.4	
Li-Muscovite ⁸	(K)(Li _{0.5} Al _{1.5})(Si ₄)O ₁₀ (OH) ₂			-5409.9	
Lepidolite ⁸	(K)(Li _{0.9} Al _{1.6})(Si _{3.3} Al _{0.7})O ₁₀ (OH) ₂			-5595.4	
Lepidolite ⁸	(K)(Li _{1.45} Al _{1.35})(Si _{3.5} Al _{0.5})O ₁₀ (OH) ₂			-5594.2	
Magnesian Mica	(K)(Mg _{2.5})(Si ₄)O ₁₀ (OH) ₂			-5578.9	
Bitiyte	(Ca)(LiAl ₂)(Si ₂ AlBe)O ₁₀ (OH) ₂			-5974.2	
Kinoshitalite-Mg	(Ba)(Mg ₃)(Si ₂ Al ₂)O ₁₀ (OH) ₂			-6083.5	
Clintonite	(Ca)(Mg ₂ Al)(SiAl ₃)O ₁₀ (OH) ₂			-6233.9	
Preiswerkite	(Na)(Mg ₂ Al)(Si ₂ Al ₂)O ₁₀ (OH) ₂			-5946.0	
Taeniolite	(K)(LiMg ₂)(Si ₄)O ₁₀ (OH) ₂			-5605.9	
Na-phlogopite	(Na)(Mg ₃)(Si ₃ Al)O ₁₀ (OH) ₂			-5801.3	

¹ Perchuk *et al.* (1981); ² Mader *et al.* (1996); ³ Holland and Powell (1990); ⁴ Chatterjee *et al.* (1998); ⁵ Martin (1994); ⁶ Miyano (1981); ⁷ Sverjensky (1985); ⁸ Ponomareva and Gordienko (1991).

parameter $\Delta_G O^=M^{z+}$ of a cation in octahedral coordination, led to two different scales of electronegativity in sites of 2:1 layers and brucitic sheets. It should be kept in mind that the general expression does not allow us to predict the excess free energies of mixing because, firstly, we have not considered the different sites M_1 to M_4 in phyllosilicates and secondly, in any interaction between two sites, the expression $X_i X_j [\Delta_G O^=M_i^{z_1+} (\text{clay}) - \Delta_G O^=M_j^{z_2+} (\text{clay})]$ is a symmetrical function.

For a model involving long-range interactions, the constancy of $\Delta_G O^=M^{z+}$ for cations in different sites is questionable and accurate results depend on the environment around the cations and protons. The influence of occupancy of cations in different sites may act on the variation of the parameter $\Delta O^=M^{z+}$ of a cation and can explain the asymmetrical behavior of the excess energy between any two consecutive sites. This step will be investigated further by using the enthalpy of formation instead of the free energies of formation.

ACKNOWLEDGMENTS

Financial support was provided by the ECOCLAY European Program (Contract N° F14WCT960032) and Agence National pour la Gestion des Dechets Radioactifs (ANDRA). The author is grateful to Professor J.D. Rimstidt and to Professor R.K. Stoessel for their careful and helpful criticisms. M.F. Hubert is thanked for her help in improving the English.

REFERENCES

- Aagard, P. and Jahren, J.S. (1992) Diagenetic illite-chlorite assemblages in arenites. II Thermodynamic relations. *Clays and Clay Minerals*, **40**, 547-554.
- Aja, S.U. and Small, J.S. (1999) The solubility of a low-Fe clinocllore between 25 and 175 degrees C and $P_v=P(H_2O)$. *European Journal of Mineralogy*, **11**, 829-842.
- Baes, C.F. and Mesmer, R.E. (1976) *The Hydrolysis of Cations*. Wiley Interscience, New York, 496 pp.
- Barin, I. (1985) *Thermochemical Data of Pure Substances, parts 1 and 2*. Verlagsgesellschaft mbH V.C.H., Germany, 1600 pp.

- Chatterjee, N.D., Kruger, R., Haller, G. and Olbricht, W. (1998) The Bayesian approach to an internally consistent thermodynamic database: theory, database, and generation of phase diagrams. *Contributions to Mineralogy and Petrology*, **133**, 149–168.
- Chermak, J.A. and Rimstidt, J.D. (1989) Estimating the thermodynamic properties (ΔG_f° and ΔH_f°) of silicate minerals at 298 K from the sum of polyhedral contributions. *American Mineralogist*, **74**, 1023–1031.
- Cox, J.D., Wagman, D.D. and Medvedev, V.A. (editors) (1989) *Codata Key Values for Thermodynamics*. Hemisphere Publishing Corp., New York, 271 pp.
- Diakonov, I.I., Pokrovski, G.S., Schott, J., Castet, S. and Gout, R. (1996) An experimental and computational study of sodium-aluminum complexing in crustal fluids. *Geochimica et Cosmochimica Acta*, **60**, 197–211.
- El-Din, A. and El-Shazly, K. (1996) Petrology of Fe-Mg-carpholite-bearing metasediments from NE Oman – Reply. *Journal of Metamorphic Geology*, **14**, 386–397.
- Gartner, L. (1979) Relations entre enthalpies ou enthalpies libres de formation des ions, des oxydes et des composés de formule $MmNnOz$. Utilisation des fréquences de vibration dans l'infra-rouge. Thèse Docteur Ingénieur, Univ. Strasbourg, France, 193 pp.
- Holland, T.J.B. and Powell, R. (1990) An enlarged and updated internally consistent thermodynamic dataset with uncertainties and correlations: the system $K_2O-Na_2O-CaO-MgO-MnO-FeO-Fe_2O_3-Al_2O_3-TiO_2-SiO_2-C-H_2O_2$. *Journal of Metamorphic Geology*, **8**, 89–124.
- Holland, T.J.B., Baker, J. and Powell, R. (1998) Mixing properties and activity-composition relationships of chlorites in the system $MgO-FeO-Al_2O_3-Fe_2O_3-SiO_2-H_2O$. *European Journal of Mineralogy*, **10**, 395–406.
- Johnson, J.W., Oelkers, E.H. and Helgeson, H.C. (1992) SUPCRT 92: A software package for calculating the standard molal thermodynamic properties of minerals, gases, aqueous species and reactions from 1 to 5000 bars and 0°C to 1000°C. *Computer Geosciences*, **18**, 899–947.
- Kittrick, J.A. (1982) Solubility of two high Mg and two high Fe chlorites using multiple equilibria. *Clays and Clay Minerals*, **30**, 167–179.
- Mader, U.K., Ramseyer, K., Daniels, E.J. and Althaus, E. (1996) Gibbs free energy of buddingtonite ($NH_4AlSi_3O_8$) extrapolated from experiments and comparison to natural occurrences and polyhedral estimation. *European Journal of Mineralogy*, **8**, 755–766.
- Martin, F. (1994) Etude cristallographique et cristallochimique de l'incorporation du germanium et du gallium dans les phyllosilicates. Approche par synthèse minérale. Thèse Docteur en Sciences, Université d'Aix Marseille, France, 210 pp.
- McPhail, D.C., Berman, R.G. and Greenwood, H.J. (1990) Experimental and theoretical constraints on aluminum substitution in magnesian chlorite, and a thermodynamic model for H_2O in magnesian cordierite. *The Canadian Mineralogist*, **28**, 859–874.
- Merceron, T., Vieillard, Ph., Fouillac, A.M. and Meunier, A. (1992) Hydrothermal alterations in the Echassiers granitic cupola (Massif Central, France). *Contributions to Mineralogy and Petrology*, **112**, 279–292.
- Mercury, L., Vieillard, Ph. and Tardy, Y. (2001) Thermodynamic of ice polymorphs and "Ice-like" water, in hydrates and hydroxides. *Applied Geochemistry*, **16**, 161–181.
- Miyano, T. (1981) Stability relations of ferri annite at Lower temperatures. *Annual Report, Institute of Geosciences, University of Tsukuba*, **8**, 95–96.
- Nriagu, J.O. (1975) Thermochemical approximation for clay minerals. *American Mineralogist*, **60**, 834–839.
- Parker, V.B. and Khodakovskii, I.L. (1995) Thermodynamic properties of the aqueous ions (2+ and 3+) of iron and the key compounds of iron. *Journal of Physical Chemical Reference Data*, **24**, 1699–1745.
- Pauling, L. (1960) *The Nature of the Chemical Bond*, 3rd edition. Cornell University Press, New York, 430 pp.
- Perchuk, L.L., Podlesskii, K.K. and Aranovich, L.Y. (1981) Calculation of thermodynamic properties of end member minerals from natural parageneses. Pp. 111–129 in: *Thermodynamics of Minerals and Melts* (R.C. Newton, A. Navrotsky and B.J. Wood, editors). Advances in Physical Geochemistry, volume 1. Springer-Verlag New York Inc.
- Pokrovskii, V.A. and Helgeson, H.C. (1995) Thermodynamic properties of aqueous species and the solubilities of minerals at high pressures and temperatures: The system $Al_2O_3-H_2O-NaCl$. *American Journal of Science*, **295**, 1255–1342.
- Ponomareva, N.I. and Gordienko, V.V.A. (1991) Physico-chemical conditions of formation of lepidolites. *Zapiski Vsesoyuznogo Mineralogicheskogo Obshchestva*, **120**, 31–39.
- Robie, R.A. and Hemingway, B.S. (1995) Thermodynamic properties of minerals and related substances at 298.15 K and 1 bar (10^5 Pascals) pressure and higher temperature. *US Geological Survey Bulletin*, Washington D.C., **2131**, 461 pp.
- Saccoccia, P.J. and Seyfried, W.E. (1993) A resolution of discrepant thermodynamic properties for chamosite retrieved from experimental and empirical techniques. *American Mineralogist*, **78**, 607–611.
- Shock, E.L. and Helgeson, H.C. (1988) Calculation of the thermodynamic properties and transport properties of aqueous species and equation of state predictions to 5 kb and 1000°C. *Geochimica et Cosmochimica Acta*, **52**, 2009–2036.
- Stoessel, R.K. (1984) Regular solution site mixing model for chlorites. *Clays and Clay Minerals*, **32**, 205–212.
- Sverjensky, D.A. (1985) The distribution of divalent trace elements between sulfides, oxides, silicates and hydrothermal solutions. I. Thermodynamic basis. *Geochimica et Cosmochimica Acta*, **49**, 853–864.
- Sverjensky, D.A., Shock, E.L. and Helgeson, H.C. (1997) Prediction of the thermodynamic properties of aqueous metal complexes to 1000°C and 5 kbar. *Geochimica et Cosmochimica Acta*, **61**, 1359–1412.
- Tardy, Y. and Duplay, J. (1992) A method of estimating the Gibbs free energies of formation of hydrated and dehydrated clays minerals. *Geochimica et Cosmochimica Acta*, **56**, 3007–3029.
- Tardy, Y. and Garrels, R.M. (1976) Prediction of Gibbs energies of formation. I. Relationships among Gibbs energies of formation of hydroxides, oxides and aqueous ions. *Geochimica et Cosmochimica Acta*, **40**, 1051–1056.
- Tardy, Y. and Garrels, R.M. (1977) Prediction of Gibbs energies of formation from the elements. II. Monovalent and divalent metal silicates. *Geochimica et Cosmochimica Acta*, **41**, 87–92.
- Tardy, Y. and Gartner, L. (1977) Relationships among Gibbs energies of formation of sulfates, nitrates, carbonates, oxides and aqueous ions. *Contributions to Mineralogy and Petrology*, **63**, 89–102.
- Tardy, Y. and Vieillard, Ph. (1977) Relation among Gibbs free energies and enthalpies of formation of phosphates, oxides and aqueous ions. *Contributions to Mineralogy and Petrology*, **63**, 75–88.
- Varadachari, C., Kudrat, M. and Ghosh, K. (1994) Evaluation of standard free energies of formation of clay minerals by an improved regression method. *Clays and Clay Minerals*, **42**, 298–307.
- Vasil'ev, V.P., Vorob'ev, P.P. and Yashkova, V.I. (1986)

- Standard enthalpy of formation of titanium ion (4+) in aqueous solution at 298.15. *Zhurnal Neorganiche Khimii*, **31**, 1869–1873.
- Vidal, O. (1997) Experimental study of the thermal stability of pyrophyllite, paragonite, and clays in a thermal gradient. *European Journal of Mineralogy*, **9**, 123–140.
- Vidal, O., Goffe, B. and Theye, T. (1992) Experimental study of the stability of sudoite and Magnesiacarpholite and calculation of a new petrogenetic grid for the system FeO–MgO–Al₂O₃–SiO₂–H₂O. *Journal of Metamorphic Geology*, **10**, 603–614.
- Vieillard, Ph. (1982) Modèle de calcul des énergies de formation des minéraux bâti sur la connaissance affinée des structures cristallines. *Sciences Géologiques Mémoire*, **69**, 206 pp.
- Vieillard, Ph. (1994a) Prediction of enthalpy of formation based on refined crystal structures of multisite compounds. 1. Theories and examples. *Geochimica et Cosmochimica Acta*, **58**, 4049–4063.
- Vieillard, Ph. (1994b) Prediction of enthalpy of formation based on refined crystal structures of multisite compounds. 2. Application to minerals belonging to the system Li₂O–Na₂O–K₂O–BeO–MgO–CaO–MnO–FeO–Fe₂O₃–Al₂O₃–SiO₂–H₂O. Results and discussion. *Geochimica et Cosmochimica Acta*, **58**, 4064–4107.
- Vieillard, Ph. (2000) A new method for the prediction of Gibbs free energies of formation of hydrated clay minerals based on the electronegativity scale. *Clays and Clay Minerals*, **48**, 459–473.
- Vieillard, Ph. and Tardy, Y. (1988a) Estimation of enthalpies of formation of minerals based on their refined crystal structures. *American Journal of Science*, **288**, 997–1040.
- Vieillard, Ph. and Tardy, Y. (1988b) Une nouvelle échelle d'électronégativité des ions dans les cristaux. Principe et méthode de calcul. *Comptes Rendus Académie Sciences Paris*, **306**, 423–428.
- Vieillard, Ph. and Tardy, Y. (1989) Une nouvelle échelle d'électronégativité des ions dans les oxydes et les hydroxydes. *Comptes Rendus Académie Sciences Paris*, **308**, 1539–1545.
- Walshe, J.L. (1986) A six component chlorite solid solution model and the conditions of chlorite formation in hydrothermal and geothermal systems. *Economic Geology*, **81**, 681–703.
- Wilcox, D.E. and Bromley, L.A. (1963) Computer estimation of heat and free energy of formation for simple inorganic compounds. *Indian Engineering Chemistry*, **55**, 32–39.
- Wolery, T.J. and Daveler, S.A. (1992) *EQ 3/6, a software package for geochemical modeling of aqueous systems*. Lawrence Livermore National Laboratory, UCRL-MA-110772 PT I-IV.
- Zolotov, M.Y., Fegley, B. and Lodders, K. (1999) Stability of micas on the surface of Venus. *Planetary Space Science*, **47**, 245–260.

(Received 5 February 2001; revised 6 December 2001; Ms. 520)